24th INTERNATIONAL CONGRESS ON SOUND AND VIBRATION
23–27 July 2017, London

ENERGY TRANSFER IN NONLINEAR VIBRATION ABSORBERS

Yu Zhang, Kefu Liu

Department of Mechanical Engineering, Lakehead University, Thunder Bay, Canada
email: kliu@lakeheadu.ca

Liuyang Xiong, Lihua Tang

Department of Mechanical Engineering, University of Auckland, New Zealand

This study is motivated to achieve simultaneous vibration suppression and energy harvesting in a broad frequency band. For this purpose, nonlinear vibration absorbers are considered. Nonlinear energy sink (NES) is a special nonlinear vibration absorber as it possesses essential nonlinear stiffness. The NES is capable of achieving targeted energy transfer (TET) that is the ability to direct vibrating energy from a source to a receiver in a one-way irreversible fashion. In this sense, the NES is considered to be weakly coupled to the primary system. This study focuses on the TET performances of a nonlinear vibration absorber coupled to three different primary systems. By varying the stiffness of the primary system, three combined systems result, namely, strongly coupled, moderately coupled, and weakly coupled. The percentage of the instantaneous energy in the absorber is used as a measure for efficacy of the TET. The nonlinear normal mode (NNM) analysis is conducted on the corresponding Hamiltonian systems. The frequency-energy plots based on the NNM analysis results and wavelet transform spectra of simulated responses are used to reveal the initial energy dependence and frequency contents in the responses. The computer simulation results show that the nonlinear vibration absorber can possess the behaviors similar to those of the NES if it is weakly coupled to the primary system.
Keywords: vibration suppression, energy harvesting, vibration absorber, nonlinear energy sink

1. Introduction

A vibration absorber is a common device to protect a host system from a harmonic excitation. When attached to the host system, the vibration absorber can suppress its steady state response if its natural frequency is tuned to be the exciting frequency. However, performance of vibration absorbers deteriorates significantly if the exciting frequency varies. Nonlinear vibration absorbers have been proposed to improve robustness in a broad frequency band [1-3]. In recent years, there has been a growing interest in harvesting energy from ambient vibration for self-powered devices. A popular way to convert vibrating energy into electricity is to use a linear oscillator. However, its performance will be compromised if ambient vibration is not sinusoidal form or harmonic exciting frequency varies from the natural frequency of the oscillator. Nonlinear oscillators have been investigated for the purpose of wide band energy harvesting [4-6]. It has been much desired to use nonlinear vibration absorbers to achieve simultaneous vibration suppression and energy harvesting.

Over the last 15 years, nonlinear energy sink (NES) technique has been gaining popularity as a better solution for broadband vibration suppression [7-9]. Unlike nonlinear vibration absorbers, the NES possesses an essential nonlinearity so that it can resonate at any frequency as long as the exciting

energy exceeds the threshold level. Many studies have shown that the NES exhibits some unique features such as targeted energy transfer (TET), 1:1 resonance, strongly modulated response (SMR), etc. and has the attractive capability of wideband vibration suppression.

In [10], an apparatus was developed for the purpose of simultaneous vibration suppression and energy harvesting in a broad band. The developed vibration absorber may be considered to be a variant NES as its stiffness contains both linear and nonlinear terms. The absorber spring was designed to keep its linear stiffness very low so that the natural frequency of the absorber was much lower than that of the primary system. The study showed that the apparatus was able to achieve the TET. In [11], the similar apparatus was used for study of piezoelectric energy harvesting. In the case of linear vibration absorbers, the ratio $\beta = \omega_a / \omega_p$ is referred to as the tuning parameter where ω_a is the natural frequency of the absorber and ω_p is the natural frequency of the primary system. A NES system may be considered to be a nonlinear vibration absorber with $\beta = 0$. This study focuses on transient performances of nonlinear vibration absorbers in terms of energy transfer. The three systems with different β values are considered. The system with $\beta = 1$ is considered to be strongly coupled, the system with $\beta = 0.5$ is considered to be moderately coupled, and the system with $\beta = 0.3$ is considered to be weakly coupled. The rest of the paper is organized as follows. Section 2 introduces the apparatus and its modelling. Section 3 presents computer simulation. Section 4 draws the study conclusions.

2. Modelling

The nonlinear vibration absorber developed in [11] is used in this study. The equations of motion for a combined system free of external excitation are defined by

$$m_p \ddot{x}_p + c_p \dot{x}_p + k_p x_p - \left[c_a \dot{z} + \left(k_1 z + k_3 z^3 \right) + \Theta V \right] = 0 \tag{1}$$

$$m_a \ddot{z} + (1+\mu)\left[c_a \dot{z} + \left(k_1 z + k_3 z^3 \right) + \Theta V \right] - \mu \left(c_p \dot{x}_p + k_p x_p \right) = 0 \tag{2}$$

where x_p and x_a represent the displacement of the primary mass and the absorber mass, respectively, m_p, c_p, and k_p are the mass, the damping coefficient, and the stiffness of the primary system, respectively, m_a and c_a are the mass and damping coefficient of the absorber, respectively, k_1 and k_3 are the linear stiffness and nonlinear stiffness of the absorber spring, respectively; $z = x_a - x_p$ is the relative displacement between the absorber mass and primary mass, $\mu = m_a / m$ is the mass ratio. The dynamics of the energy harvesting circuit is defined by

$$V / R + C^S \dot{V} - \Theta \dot{z} = 0 \tag{3}$$

where Θ is the electromechanical coupling coefficient of the PEH; V is the voltage across the load resistor whose resistance is R and; C^S is the capacitance of the PEH.

In order to investigate energy transfer from the primary system to the absorber system, the percentage of the instantaneous energy in the absorber is defined as

$$D(t) = \frac{E_a(t)}{E_p(t) + E_a(t)} \times 100\% \tag{4}$$

where $E_a(t)$ is the instantaneous energy in the absorber at time t and defined as

$$E_a(t) = \frac{m_a \dot{x}_a(t)^2}{2} + \frac{k_1 [x_a(t) - x_p(t)]^2}{2} + \frac{k_3 [x_a(t) - x_p(t)]^4}{4} \tag{5}$$

and $E_p(t)$ is the total energy in the primary system at time *t* and defined as

$$E_p(t) = \frac{1}{2} m_p \dot{x}_p(t)^2 + \frac{1}{2} k_p x_p(t)^2 \tag{6}$$

In addition, the accumulated energy harvested by the PEH is defined as

$$E_h(t) = \int_0^t V(t)^2 / R dt \tag{7}$$

In order to determine an initial energy threshold required to engage the absorber mass into 1:1 resonance, a nonlinear normal mode (NNM) analysis [7] is conducted. For this purpose, the underlying Hamiltonian system is considered

$$m_p \ddot{x}_p + k_p x_p - k_1 z - k_3 z^3 = 0 \tag{8}$$

$$m_a \ddot{z} + (1+\mu)(k_1 z + k_3 z^3) - \mu k_p x_p = 0 \tag{9}$$

The NNM analysis starts with defining complex variables as follows

$$\psi_1 = \dot{x}_p + j\omega x_p \text{ and } \psi_2 = \dot{x}_a + j\omega x_a \tag{10}$$

where ω is the dominant frequency or also known as the fast oscillating frequency and $j = \sqrt{-1}$. By rearranging these new complex variables, displacements and accelerations of the primary system and absorber system are obtained as

$$x_p = \frac{\psi_1 - \overline{\psi}_1}{2j\omega}, \ \ddot{x}_p = \dot{\psi}_1 - \frac{j\omega}{2}(\psi_1 + \overline{\psi}_1) \tag{11}$$

$$x_a = \frac{\psi_2 - \overline{\psi}_2}{2j\omega}, \ \ddot{x}_a = \dot{\psi}_2 - \frac{j\omega}{2}(\psi_2 + \overline{\psi}_2) \tag{12}$$

where the overhead bar represents complex conjugate. Since periodic orbits are sought, it is assumed that the primary system and absorber oscillate with the same fast frequency ω, the previously defined complex variables in Equation (10) are approximately expressed in terms of the fast frequency ω, $e^{j\omega t}$ and modulated by slowly varying amplitudes $\phi_i(t)$, $i = 1, 2$ as

$$\psi_1(t) = \phi_1(t) e^{j\omega t} \text{ and } \psi_2(t) = \phi_2(t) e^{j\omega t} \tag{13}$$

Substituting Eqs. (11), (12), and (13) into Eqs. (8) and (9) and simplifying them by neglecting higher order terms associated with $e^{j3\omega t}$ and $e^{j5\omega t}$ result in

$$m_p\left(\dot{\phi}_1 + \frac{j\omega}{2}\phi_1\right) - \frac{jk_p}{2\omega}\phi_1 + \frac{jk_1}{2\omega}(\phi_2 - \phi_1) + \frac{3jk_3}{8\omega^3}\left(\phi_1^2\overline{\phi}_2 - \overline{\phi}_1\phi_2^2 - \overline{\phi}_1\phi_1^2 + \phi_2^2\overline{\phi}_2 - 2\phi_1\phi_2\overline{\phi}_2 + 2\phi_1\overline{\phi}_1\phi_2\right) = 0 \tag{14}$$

$$\begin{aligned} &m_a\left[\left(\dot{\phi}_2 + \frac{j\omega}{2}\phi_2\right) - \left(\dot{\phi}_1 + \frac{j\omega}{2}\phi_1\right)\right] + \frac{j\mu k_p}{2\omega}\phi_1 - \frac{jk_1}{2\omega}(1+\mu)(\phi_2 - \phi_1) \\ &- \frac{3jk_3}{8\omega^3}(1+\mu)\left(\phi_1^2\overline{\phi}_2 - \overline{\phi}_1\phi_2^2 - \overline{\phi}_1\phi_1^2 + \phi_2^2\overline{\phi}_2 - 2\phi_1\phi_2\overline{\phi}_2 + 2\phi_1\overline{\phi}_1\phi_2\right) = 0 \end{aligned} \tag{15}$$

where dot denotes the derivative with respect to time. Furthermore, a polar form of complex amplitudes is introduced as $\phi_1 = a(t)e^{j\alpha(t)}$ and $\phi_2 = b(t)e^{j\gamma(t)}$, where $a(t)$ and $b(t)$ are real amplitudes and $\alpha(t)$ and $\gamma(t)$ are real phases. Substituting them into Eqs. (14) and (15) and separating the real and imaginary parts yield four first-order differential equations about variables a, α, b, and γ [9]. Since periodic solutions are sought, the four first-order differential equations become four coupled

nonlinear algebraic equations by letting the derivatives of a , α , b , and γ be zero. Furthermore, the system is assumed to oscillate in phase $\alpha = \gamma$, a set of two coupled nonlinear algebraic equations result

$$\frac{-9k_3a^2b - 3k_3b^3 - 4k_1b\omega^2 + 4k_pa\omega^2 - 4m_pa\omega^4 + 4k_1a\omega^2 + 3k_3a^3 + 9k_3ab^2}{8m_pa} = 0 \tag{16}$$

$$\frac{-9k_3ab^2 - 3k_3a^3 - 4k_1a\omega^2 + 4k_1b\omega^2 - 4m_ab\omega^4 + 3k_3b^3 + 9k_3a^2b}{8m_ab} = 0 \tag{17}$$

The two equations are numerically solved for a and b by specifying a frequency ω. If $a > 0$ and $b > 0$, the system is in in-phase motion while if $a < 0$ and $b > 0$ the system is in out-of-phase motion. In general, the periodic responses can be expressed as follows

$$x_p(t) \approx \frac{\psi_1 - \bar{\psi}_1}{2j\omega} = X_p\cos(\omega t),\ x_a(t) \approx \frac{\psi_2 - \bar{\psi}_2}{2j\omega} = X_a\cos(\omega t) \tag{18}$$

where $X_p = a/\omega$ and $X_a = b/\omega$. As the system is Hamiltonian, its total energy is equal to its potential energy defined as

$$E = \frac{1}{2}k_pX_p^2 + \frac{1}{2}k_1Z^2 + \frac{1}{4}k_3Z^4 \tag{19}$$

where $Z = X_a - X_p$.

3. Computer Simulation

In order to define level of coupling between the primary system and the absorber system, Eqs. (1) , (2), and (3) are reformulated by defining a dimensionless time $\tau = \omega_p t$ as

$$x_p'' + 2\zeta_p x_p' + x_p - 2\mu\zeta_a\beta z' - \mu\beta^2 z - \bar{k}_3 z^3 - \bar{\theta}V = 0 \tag{20}$$

$$z'' + (1+\mu)\left(2\zeta_a\beta z' + \beta^2 z + \frac{1}{\mu}\bar{k}_3 z^3 + \frac{1}{\mu}\bar{\theta}V\right) - 2\zeta_p x_p' - x_p = 0 \tag{21}$$

$$\frac{V}{k_p\omega_p R} + \frac{C^S}{k_p}V' - \bar{\theta}z' = 0 \tag{22}$$

where

$$\beta = \frac{\omega_a}{\omega_p},\ \bar{k}_3 = \frac{k_3}{k_p},\ \bar{\theta} = \frac{\Theta}{k_p},\ \omega_p = \sqrt{\frac{k_p}{m_p}},\ \omega_a = \sqrt{\frac{k_1}{m_a}},\ \zeta_p = \frac{c_p}{2m_p\omega_p},\ \zeta_a = \frac{c_a}{2m_a\omega_a}$$

and prime represents derivative with respect to τ . Note that the variable β is referred to as the tuning ratio [12]. In the case of linear vibration absorbers, $\beta = 1$ is referred to as constant tuning. In the case of nonlinear vibration absorbers, if $\beta = 0$, the system becomes a true NES whereas if $\beta = 1$, the system becomes a traditional nonlinear vibration absorber. In what follows, three systems will be considered by varying the tuning ratio. With $\beta_1 = 0.3$, the absorber is weakly coupled to the primary system. With $\beta_2 = 0.5$, the absorber is moderately coupled to the primary system. With $\beta_3 = 1.0$, the absorber is strongly coupled to the primary system. In simulation, the following parameters are kept constants with the values

$m_p = 0.839$ kg, $\zeta_p = 0.01$, $m_a = 0.0307$ kg, $\zeta_a = 0.01$, $k_1 = 25.53$ N/m, $k_3 = 1.979 \times 10^7$ N/m^3
$C^S = 8.39 \times 10^{-10}$ F, $\theta = 1.296 \times 10^{-4}$ N/V, $R =$ 100 KΩ

The procedure to identify the above parameter values can be found in [11]. The linear natural frequency of the absorber is $f_a = \sqrt{k_1/m_a}/2\pi = 4.5$ Hz. Using the specified β values, it is found that $f_{p1} = 15.0$ Hz, $f_{p2} = 9.0$ Hz, and $f_{p3} = 4.5$ Hz, respectively. Thus, $k_{p_1} = 7.752 \times 10^3$ N/m, $k_{p_2} = 2.791 \times 10^3$ N/m, and $k_{p_3} = 6.977 \times 10^2$ N/m, respectively. The system is assumed to be released from an initial condition $x_p(0) = x_a(0) = X$, $\dot{x}_p(0) = 0$, $\dot{x}_a(0) = 0$. To have a fair comparison, the free responses are generated by keeping the initial potential energy constant. Therefore, the initial displacement for each of the three systems is determined by

$$X_i = \sqrt{\frac{2E(0)}{k_{pi}}}, \quad i = 1,\ 2,\ 3 \tag{23}$$

where $E(0)$ is the specified initial energy.

Figure 1 shows the time responses with $E(0) = 2.736 \times 10^{-2}$ J. The corresponding initial displacements are $X_1 = 2.67$ mm, $X_2 = 4.45$ mm, $X_3 = 8.90$ mm, respectively. As shown in Fig. 1 (a), for the weakly coupled system, the energy is quickly localized in the absorber mass and the TET is established. On the other hand, as shown in Fig. 1(e), for the strongly coupled system, the energy transfer does not occur and the TET is not activated. As shown in Figs. 1(b) and 1(f), the output voltage of the weakly coupled system is greater than that of the strongly coupled system. Figure 2 shows the corresponding percentages of the instantaneous energy in the absorber system and the ratio of the accumulated harvested energy to the initial energy. It is shown that the weakly coupled system has the fastest energy transfer from the primary system to the absorber system among the three systems. It is also shown that the PEH output voltage of the weakly coupled system is greatest among the three systems.

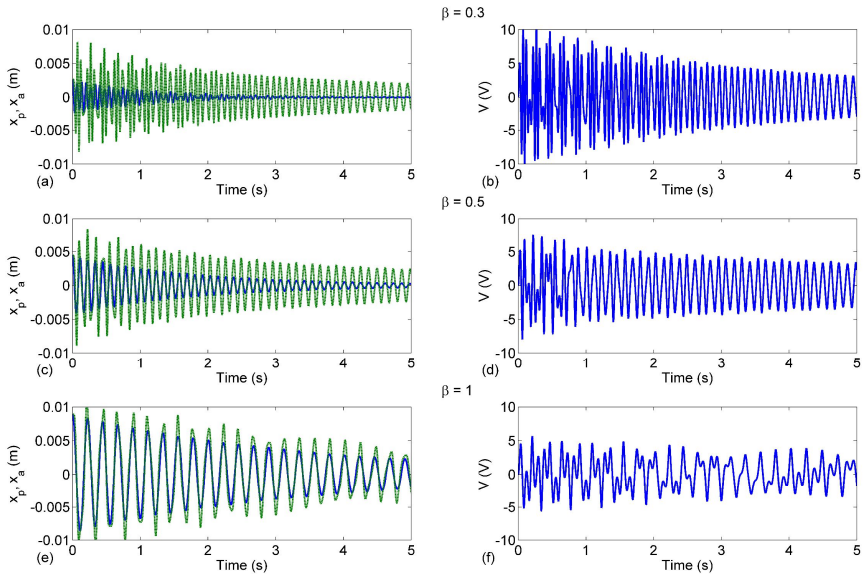

Figure 1: Time responses of the systems with $E(0) = 2.736 \times 10^{-2}$ J, (a) and (b) $\beta_1 = 0.3$; (c) and (d) $\beta_2 = 0.5$; (e) and (f) $\beta_3 = 1.0$. $x_p(t)$ (blue solid line), $x_a(t)$ (green dotted line).

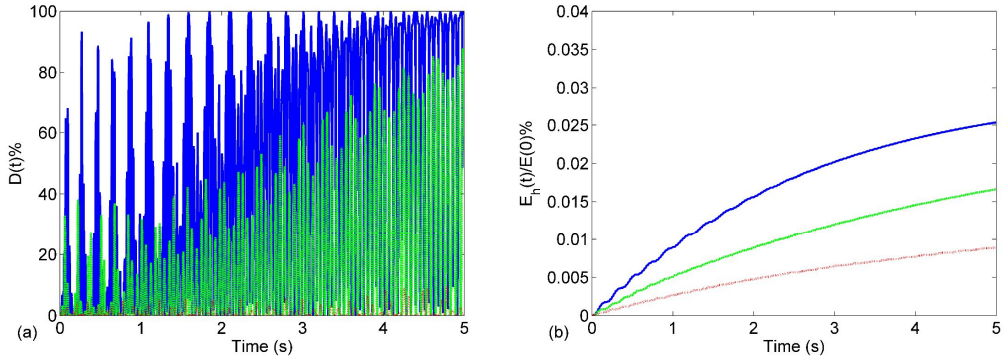

Figure 2: Simulation results with $E(0) = 2.736 \times 10^{-2}$ J, (a) the percentages of the instantaneous energy of the absorber system defined by Eq. (4); (b) the ratio of the accumulated harvested energy to the initial energy: blue solid line for $\beta_1 = 0.3$; green dotted line for $\beta_2 = 0.5$; red dashed line for $\beta_3 = 1.0$.

Figures 3 and 4 are the so-called frequency-energy plots for the cases $\beta_1 = 0.3$ and $\beta_2 = 0.5$, respectively. In the figures black solid lines represent the two backbone branches computed by Eq. (19) based on the results of the NNM analysis. The in-phase branch is denoted by S11+ while the out-of-phase branch is denoted by S11-. The coloured areas represent the contour plots of the wavelet transform (WT) spectra obtained using the relative displacements from computer simulation. In the figures, the four initial energy (IE) levels correspond to low-IE, medium-IE, medium-high-IE, and high-IE, respectively. As shown in the figures, the S11+ backbone branch originates from the first natural frequency of the linearized system while the S11- backbone branch starts from the second natural frequency of the linearized system. The ET indicated in the figures represents the energy threshold. For a true NES or $\beta = 0$, the ET marks the beginning of 1:1 resonance and energy transfer from the primary mass to the NES mass. If the initial energy level exceeds the ET, the NES mass is set into oscillation in the frequency of the primary system. As a result, the responses are attracted to the S11+ branch and the desired TET is established. If the IE is lower than the ET, the responses will be attracted to the S11- branch and the TET cannot be achieved [9]. In the case of $0 < \beta < 1$, decreasing the β value will move the S11- branch up and the ET to the right. This results in a strong nonlinear behaviour and energy concentration on the S11+ branch if the IE reaches the ET, as indicated in Figs. 3(c) and 3(d). On the other hand, increasing the β value will move the S11- branch down and the ET to the left. As the result, less IT is required to engage the absorber mass in 1:1 resonance. However, the responses exhibit a weak nonlinear behaviour since the 1:1 resonance frequency is low as indicated in Figs. 4(b), 4(c), and 4(d). Due to a coupling between the primary system and absorber system, the TET or the one-way irreversible energy transfer is not fully established. The results shown in Fig. 3 reveal that when the nonlinear vibration absorber is weakly coupled to the primary system, it behaves similarly as the NES.

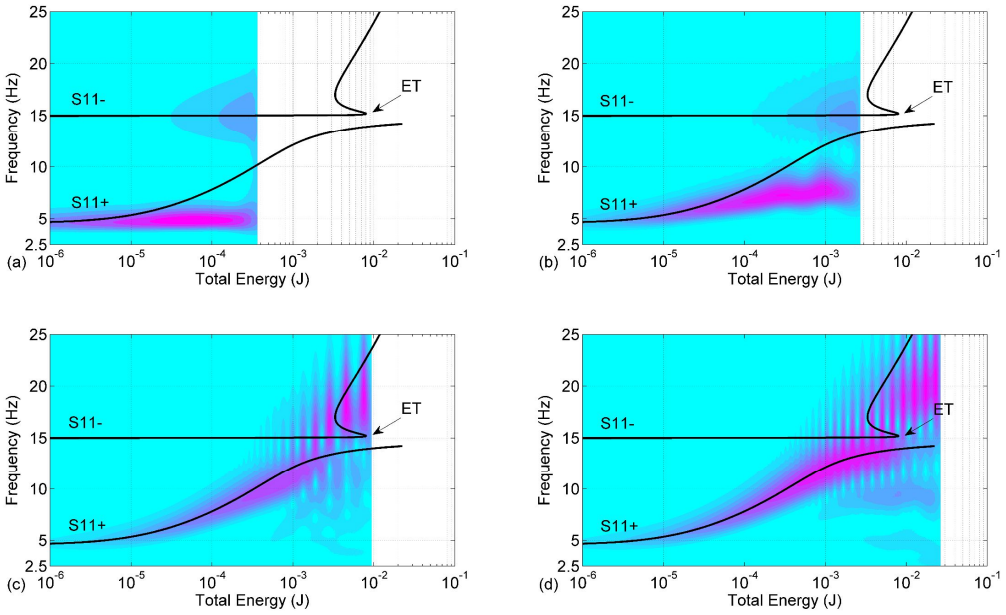

Figure 3: Frequency-energy plots for the system with $\beta_1 = 0.3$, (a) low-IE $E(0) = 3.773\times10^{-4}$ J; (b) medium-IE $E(0) = 2.814\times10^{-4}$ J; (c) medium-high-IE $E(0) = 9.800\times10^{-3}$ J; and (d) high-IE $E(0) = 2.763\times10^{-2}$ J.

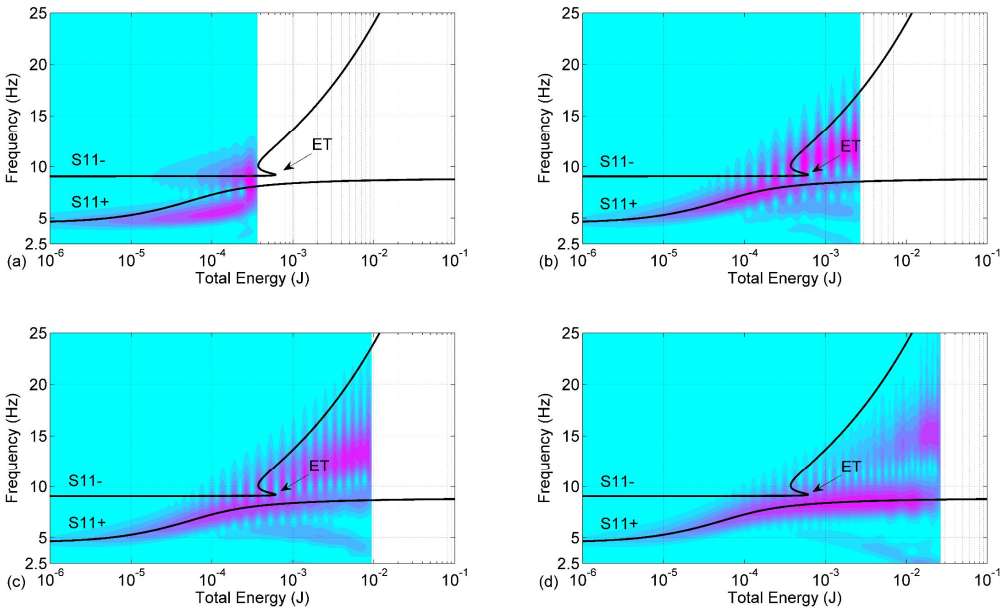

Figure 4: Frequency-energy plots for the system with $\beta_2 = 0.5$, (a) low-IE $E(0) = 3.773\times10^{-4}$ J; (b) medium-IE $E(0) = 2.814\times10^{-4}$ J; (c) medium-high-IE $E(0) = 9.800\times10^{-3}$ J; and (d) high-IE $E(0) = 2.763\times10^{-2}$ J.

4. Conclusion

This study has investigated vibration suppression and energy harvesting using a nonlinear vibration absorber. The focus has been placed on energy transfer from the primary system to the absorber system in transient responses. The nonlinear vibration absorber under consideration possesses a strong hardening nonlinearity. By fixing the absorber system and varying the stiffness of the primary system, three systems, namely weakly coupled, moderately coupled, and strongly coupled, have been investigated. The percentage of the instantaneous energy in the absorber has been used as a measure for efficacy of energy transfer. The ratio of the accumulated harvested energy to the initial energy has been used as a measure for efficacy of energy harvesting. The nonlinear normal mode (NNM) analysis has been conducted on the corresponding Hamiltonian system. The frequency-energy plots based on the NNM analysis results and wavelet transform spectra of the simulated responses have been used to reveal the initial energy dependence and frequency contents in the responses. Based on the study, the following observations can be drawn. The weakly coupled system requires a high initial energy threshold to achieve the targeted energy transfer (TET). For the simulation cases considered, the energy threshold required by the weakly coupled system is about 30% greater than that required by the moderately coupled system. However, as soon as the initial energy exceeds the energy threshold, the weakly coupled system demonstrates a better TET performance than the other two systems, indicated by a quick energy localization in the absorber mass. As the result, the absorber can quickly suppress the vibration of the primary system and the piezoelectric energy harvester is able to produce a high output voltage. For the simulation cases considered, the ratio of the accumulated harvested energy to the initial energy from the weakly coupled system is 5 times greater than that from the strongly coupled system. The study has shown that the nonlinear vibration absorber can possess the behaviours similar to those of the NES if it is weakly coupled to the primary system.

REFERENCES

1 Hunt, J. and Nissen, C. The Broadband Dynamic Vibration Absorber, *Journal of Sound and Vibration*, **83** (4), 573–578, (1982).

2 Nissen, J., Popp, K., and Schmalhorst, B. Optimization of Non-linear Dynamic Vibration Absorber, *Journal of Sound and Vibration*, **99** (1), 149–154, (1985).

3 Oueini, S. and Nayfeh, A. Analysis and Application of a Nonlinear Vibration Absorber, *Journal of Vibration Control*, **6** (7), 999-1016, (2000).

4 Gammaitoni, L., Neri, I. and Vocca, H. Nonlinear Oscillators for Vibration Energy Harvesting. *Applied Physics Letters* **94**, 164102, (2009).

5 Daqaq, M. Response of Uni-modal Duffing-type Harvesters to Random Forced Excitations, *Journal of Sound and Vibration*, **329** (18), 3621–3631, (2010).

6 Elvin, N. and Erturk, A. *Advances in Energy Harvesting Methods*, Springer, New York, (2013).

7 Gendelman, O., Manevitch, L., Vakakis, A., and M'Closkey, R. Energy Pumping in Nonlinear Mechanical Oscillators: part I – Dynamics of the Underlying Hamiltonian Systems, *Journal of Applied Mechanics*, **68** (1), 34–41, (2001).

8 Vakakis, A. and Gendelman, O. Energy Pumping in Nonlinear Mechanical Oscillators: part II – Resonance Capture, *Journal of Applied Mechanics*, **68** (1), 42–48, (2001).

9 Vakakis, A., Gendelman, O., Bergman, L., McFarland, D., Kerschen, G., and Lee, Y., Nonlinear Targeted Energy Transfer in Mechanical and Structural Systems, Springer, New York (2008).

10 Kremer, D. and Liu, K., A Nonlinear Energy Sink with an Energy Harvester: Transient Responses, *Journal of Sound and Vibration*, **333** (20), 4859-4880, (2014)

11 Zhang, Y., Tang, L., and Liu, K., Piezoelectric Energy Harvesting with a Nonlinear Energy Sink, *Journal of Intelligent Material Systems and Structures*, DOI:10.1177/1045389X16642301, (2016).

12 Den Hartog, A. *Mechanical Vibrations*, McGraw-Hill, New York, (1956).